Journal of Applied Mechanics and Technical Physics, Vol. 38, No. 2, 1997

APPLICATION OF A HIGH-VISCOSITY LIQUID TO A MOVING BASE

V. M. Shapovalov

UDC 678.027:532.522

Kochin [1] studied the static balance of a nonextensible heavy filament in the problem of the kite-balloon thread shape under the action of wind. Krylov [2] studied the problem of the balance conditions of a spherical mine in flow. Entov and Yarin [3] analyzed numerous physical phenomena typical of the dynamics of free jets and dropping-liquid films. One of the latest studies of dynamic phenomena in rectilinear jets was performed by Yarin [4]. The static balance of a bent jet of a high-viscosity liquid was analyzed for the first time by Entov et al. [5]. Shapovalov [6–8] studied the physical effects typical of such a flow.

In the present paper, we study the effect of flow conditions on the kinematic parameters of a steady, gravitationally bent jet in the long-wave approximation. The steady-flow region was determined by numerical analysis of the linearized problem of jet perturbations. The results can be used to form films by "pouring" polymer melts [9] and solutions [10] on a moving base or a rotating roll. Furthermore, the flow considered is used in the technology of light-sensitive materials. To intensify these processes and increase the film quality (e.g., by eliminating the difference in longitudinal film thickness), it is necessary to understand the regularities in the flow of a gravitationally bent, strained jet.

1. Formulation of the Problem. The stream lines and the coordinates system are shown in Fig. 1. A high-viscosity liquid jet is continuously squeezed out from the plane slot 1, the initial jet velocity being the same across the slot width. Below the forming device, the plane base 2 moves with a constant velocity v_1 in the horizontal direction (surface roughness and roll curvature are ignored). At the instant the jet touches the surface, the strains in the jet cease, and the liquid begins to move with a velocity v_1. Air suction into the clearance between the liquid and the base [11] is ignored.

The origin of the Cartesian coordinates is located at the center of the jet section at which the change in the velocity profile is completed. The x axis is horizontal, and the y axis is vertical. The x, y coordinates characterize the location of the median surface. The dot-and-dashed curve shows the median surface whose extent is designated by s. Bending occurs in the xy plane. The values $x = l$ and $y = -h$ correspond to the point of "sticking" of the jet to the surface. The physical point of contact lies below half the finite thickness of the jet. The current section of the jet is of thickness δ and width b, and the normal section of the jet at the beginning of the coordinate system is a rectangle with dimensions b_0 and δ_0.

The jet liquid flow is studied using a quasi-one-dimensional description ignoring the inertial, capillary, and aerodynamic (air friction) forces, which are small in comparison with the viscous force. The jet thickness is small compared with its length, and, hence, the bending moment is insignificant. We consider the median surface of the jet as a one-dimensional material continuum (parameters are averaged over the jet thickness and width). In this case, we have the equations

$$\frac{\partial b\delta}{\partial t} + \frac{\partial b\delta v}{\partial s} = 0, \quad \frac{\partial}{\partial s}(b\delta\sigma_{11}\cos\varphi) = 0, \quad \frac{\partial}{\partial s}(b\delta\sigma_{11}\sin\varphi) = b\delta\rho g, \quad \frac{\partial y}{\partial s} = \sin\varphi, \quad \frac{\partial x}{\partial s} = \cos\varphi. \tag{1.1}$$

The initial and boundary conditions for Eqs. (1.1) are

$$\begin{aligned} &t = 0: \quad \delta = \delta_*(s), \quad v = v_*(s), \quad y = y_*(s), \quad x = x_*(s), \\ &t > 0: \quad x = 0, \quad y = 0, \quad v = v_0, \quad \varphi = \varphi_0, \quad \delta = \delta_0, \quad s = 0, \\ &t > 0: \quad x = l, \quad y = -h, \quad v = v_1, \quad \varphi = 0, \quad s = s_+. \end{aligned} \tag{1.2}$$

Polytechnic Institute of the Volgograd State Technical University, Volgograd 404121. Translated from Prikladnaya Mekhanika i Tekhnicheskaya Fizika, Vol. 38, No. 2, pp. 170–175, March–April, 1997. Original article submitted September 19, 1995; revision submitted December 5, 1995.

Here t is time, φ is the angle between the tangent to the jet trajectory and the horizontal, ρ is the liquid density, g is the acceleration of gravity, v is the velocity, φ_0 is the initial angle, s_+ is the total length of the unperturbed jet, and v_0 is the initial velocity. In the general case, the parameters v_0, h, v_1, s_+, l, φ_0, and δ_0 can be functions of time.

In system (1.1), the first equation is the continuity equation, the second and third equations are the projections of the momentum equation, and the forth and fifth equations are geometrical ratios. In the case of a round jet, it suffices to substitute πr^2 (r is the jet radius) for $b\delta$ in (1.1).

To close the problem, it is necessary to determine the stretching stresses. We assume that the strain rates are insignificant, and the liquid properties can be described by the Newton law $\sigma = -p\delta + 2\eta d$, where p is the isotropic pressure, η is viscosity, δ is a metrical tensor, and σ and d are the stress and strain-rate tensors.

Let us designate the stress-tensor components as σ_{11}, σ_{22}, and σ_{33} (the subscript 1 indicates the tangent unit vector to the jet axis, the subscript 2 indicates the binormal unit vector, and the subscript 3 indicates the normal unit vector). If the air friction on the surface of a high-viscosity, dropping-liquid jet with long-wave disturbances is ignored, the stresses σ_{21} and σ_{31} in the jet are much smaller than the axial stress σ_{11}: $\sigma_{21} = O(\varepsilon\sigma_{11})$ and $\sigma_{31} = O(\varepsilon\sigma_{11})$, where $\varepsilon \sim \delta_0/s_+ \ll 1$. The small values of tangential stresses indicate that the flowing jet cross section remains plane under jet bending. Therefore, the parallelepiped that can be mentally cut from a rectangular jet bends with the jet and is extended along the jet axis s, preserving a rectangular section. This pattern does not change with an increase in the disturbance amplitude as long as the long-wave motion pattern is sustained and until jet sections of large curvature appear. The latter occurs only at very high amplitudes of disturbances.

For the flow of a plane jet applied to a moving surface, e.g., a rotating roll, a "widening" effect is observed: the jet width increases with decrease in the length of the flow zone. This effect results from the liquid friction on the surface [12]. Under uniaxial tension conditions $\sigma_{22} = \sigma_{33} = 0$, the transverse strain of the liquid section is isotropic (the cross sections are geometrically similar). The jet width does not change only when the external stress $\sigma_{22} = \sigma_{11}/2$ is applied to the jet edges. Shapovalov and Tyabin [13] proposed simulating the effect of the jet friction on the roll surface by applying stretching stresses to the jet edges, i.e., $\sigma_{33} = 0$ and $\sigma_{22} = \psi\sigma_{11}$, where ψ is a coefficient that depends on the flow-zone dimensions ($0 \leqslant \psi \leqslant 0.5$).

In the general case, the rheodynamics of a plane jet is characterized by the ratios $d_{11} = v' = dv/ds$, $d_{22} = v'(2\psi - 1)/(2-\psi)$, $d_{33} = v'(1+\psi)/(\psi - 2)$, $p = 2\eta v'(1+\psi)/(\psi-2)$, and $\sigma_{11} = 6\eta v'/(2-\psi)$. According to [13], for $s_+ > b_0$, uniaxial flow is observed ($\psi = 0$ and $\sigma_{11} = 3\eta v'$). Technological processes [9, 10] are characterized by relatively short jets ($s_+ \ll b_0$), and, hence, we assume that $\sigma_{11} = 4\eta v'$, $b = b_0$, and $\psi = 0.5$.

2. Steady Flow. Under steady-flow conditions ($\partial/\partial t = 0$), the continuity equation reduces to the ratio $v_0\delta_0 = v\delta$. Choosing δ_0, v_0, h/v_0, and h as scales for δ, v, t, and linear dimensions, respectively, we write problem (1.1) and (1.2) in dimensionless form as

$$\bar\delta V = 1, \quad \frac{d}{d\bar s}\Big(\bar\delta\frac{dV}{d\bar s}\cos\varphi\Big) = 0, \quad \frac{d}{d\bar s}\Big(\bar\delta\frac{dV}{d\bar s}\sin\varphi\Big) = R\bar\delta, \quad \frac{dY}{d\bar s} = \sin\varphi, \quad \frac{dX}{d\bar s} = \cos\varphi,$$
$$X = 0\colon\ \ Y = 0, \quad V = 1, \quad \varphi = \varphi_0, \quad \bar\delta = 1, \quad \bar s = 0, \tag{2.1}$$
$$X = L\colon\ \ Y = -1, \quad V = K, \quad \varphi = 0, \quad \bar s = \bar s_+.$$

Let us introduce the dimensionless parameters

$$\bar\delta = \frac{\delta}{\delta_0}, \quad V = \frac{v}{v_0}, \quad K = \frac{v_1}{v_0}, \quad R = \frac{\rho g h^2}{4\eta v_0}, \quad \tau = \frac{t v_0}{h}, \quad \{X, Y, L, \bar s, \bar s_+\} = \{x, y, l, s, s_+\}/h. \tag{2.2}$$

According to the second equation in (2.1), the horizontal tension component is constant along the jet length $[(V^{-1}dV/d\bar s)\cos\varphi = H$, where $H = \text{const}$ (Fig. 1)].

The solution of problem (2.1) is represented in parametric form:

$$(1 - 1/V)R/H^2 = 0.5[T(\varphi) - T(\varphi_0)], \quad T(\varphi) = \tan\varphi\sec\varphi + \ln|\sec\varphi + \tan\varphi|,$$
$$\frac{XR}{H} = \int_{\varphi_0}^{\varphi}\frac{V\,d\varphi}{\cos\varphi}, \qquad \frac{YR}{H} = \int_{\varphi_0}^{\varphi}\frac{V\tan\varphi\,d\varphi}{\cos\varphi}, \qquad \frac{\bar s R}{H} = \int_{\varphi_0}^{\varphi}\frac{V\,d\varphi}{\cos^2\varphi}. \tag{2.3}$$

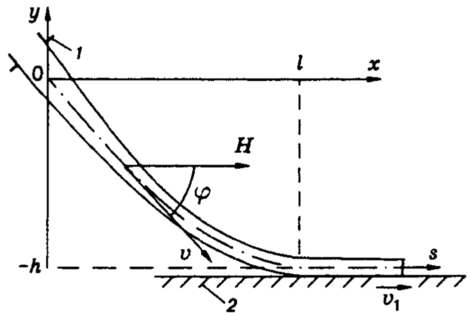

Fig. 1

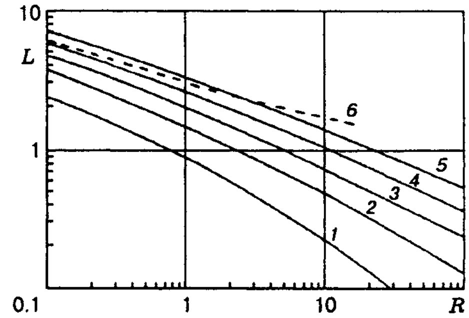

Fig. 2

For specified K and φ_0, the constants R, H, L, and $\bar{s}_+$ are determined from the relations

$$R = -\frac{2(K-1)}{KT(\varphi_0)}\Big(-\int\limits_{\varphi_0}^{0}\frac{V\sin\varphi\,d\varphi}{\cos^2\varphi}\Big)^2, \qquad 2R(K-1) = -H^2KT(\varphi_0),$$
$$\frac{LR}{H} = \int\limits_{\varphi_0}^{0}\frac{V\,d\varphi}{\cos\varphi}, \qquad \frac{R}{H} = -\int\limits_{\varphi_0}^{0}\frac{V\tan\varphi\,d\varphi}{\cos\varphi}, \qquad \frac{\bar{s}_+R}{H} = \int\limits_{\varphi_0}^{0}\frac{V\,d\varphi}{\cos^2\varphi}. \tag{2.4}$$

The results of the analysis of (2.4) are shown in Fig. 2 as curves of L versus R for $K = 2$, 4, 8, 16, and 32 (curves 1–5) [curve 6 is a bifurcation curve (see Sec. 3)]. The distance to the point of the jet contact with the roll surface increases as K increases and R decreases. The curve of $L(R, K)$ is monotonic and has no extremes. The condition $H > 0$ is satisfied for $K > 1$. The region $2 \leqslant K \leqslant 256$, $-\pi/12 \geqslant \varphi_0 \geqslant -\pi/2 + 0.05$, $10^{-3} \lesssim R \lesssim 10^3$, and $0.2 \lesssim H \lesssim 2$ was studied.

Analysis of (2.3) shows that the axial-velocity distribution along the jet length depends greatly on R. Thus, for large R, intense stretching occurs in the initial "vertical" jet section, and for small R, it is observed at the end of the flow zone, in the vicinity of the contact point.

For $\varphi = -\pi/2$, the solution of the problem has an infinite discontinuity due to the cofactor $\sec\varphi$ in Eqs. (2.3) and (2.4). Therefore, the region of steady jet configurations is limited by the sector $-\pi/2 < \varphi < 0$. Neglect of the bending moment in Eqs. (1.1) is apparently responsible for this limitation.

3. Numerical Study of Stability. Upon stretching, e.g., in synthetic-fiber forming, a rectilinear jet becomes unsteady when the extension ratio reaches a critical value [3, 4]. In this case, periodic fluctuations of the jet radius, tension, and velocity arise. This phenomenon is called "stretching resonance." Steady isothermic flow is unsteady when the extension ratio exceeds the critical value equal to 20.22. The loss of stability results in the occurrence of a new cycle — excitation of self-oscillations.

In a closed system, the oscillation intensity can spontaneously increase in the presence of an external-energy source. The jet receives energy from a translationally moving base. The occurrence of self-oscillations with an increasing amplitude is typical of systems with positive feedback. With any jet disturbance, the information on the variation in the outlet section returns to the flow zone as a stretching force that synchronously varies with time and is uniform over the jet length (the capillary and inertial forces are ignored). The stretching-force fluctuations modulate the dynamic processes in the jet. This activates oscillations whose period is close to the residence time of a liquid particle in the flow zone.

The stretching force is proportional to the product of the cross-sectional area by the gradient of the outlet strain-rate. For a rectilinear jet of a viscous liquid, the strain-rate gradient is maximal at the suction point (an exponential distribution of the axial velocity). Any method of decreasing the rate gradient at the suction point (nonisothermicity and dilatancy) extends the steady-flow region. In the case of a bent jet, the additional degree of freedom changes the dynamic properties of the jet.

Let us introduce small perturbations of thickness, velocity, slope, and vertical deviations:

$$\bar{\delta} = \bar{\delta}_*(\bar{s})[1 + \alpha(\tau, \bar{s})], \quad V = V_*(\bar{s})[1 + \beta(\tau, \bar{s})], \tag{3.1}$$

$$\varphi = \varphi_*(\bar{s}) + \gamma(\tau, \bar{s}), \qquad Y = Y_*(\bar{s}) + \xi(\tau, \bar{s}), \qquad \max(\alpha, \beta, \gamma, \xi) \ll 1.$$

Here and below, the quantities corresponding to a steady flow are designated by an asterisk; the $\bar{s}$ axis is "frozen" in the unperturbed jet.

For the moment $\tau = 0$, the unperturbed jet is described by the equations

$$\bar{\delta}_* V_* = 1, \quad \frac{d\varphi_*}{d\bar{s}} = \frac{R\cos^2\varphi_*}{HV_*}, \quad \frac{dV_*}{d\bar{s}} = \frac{HV_*}{\cos\varphi_*}, \quad \frac{dY_*}{d\bar{s}} = \sin\varphi_*,$$
$$\bar{s} = 0: \quad \varphi_* = \varphi_{*0}, \quad V_* = 1, \quad Y_* = 0, \qquad \bar{s} = \bar{s}_+: \quad \varphi_* = 0, \quad V_* = K, \quad Y_* = -1. \tag{3.2}$$

Considering simultaneously (1.1), (1.2), (2.2), (3.1), and (3.2) and linearizing them, we obtain the following equations for the deviations:

$$\frac{\partial\alpha}{\partial\tau} + V_*\frac{\partial\alpha}{\partial\bar{s}} + V_*\frac{\partial\beta}{\partial\bar{s}} = 0, \quad \beta R\cos\varphi_* + \frac{HV_*}{\cos\varphi_*}\frac{\partial\gamma}{\partial\bar{s}} + \frac{R\cos^2\varphi_*}{H}\frac{\partial\beta}{\partial\bar{s}} + \gamma R\sin\varphi_* = 0,$$
$$\sin\varphi_*\frac{\partial^2\beta}{\partial\bar{s}^2} + \left(\frac{R\cos^3\varphi_*}{HV_*} + H\tan\varphi_*\right)\frac{\partial\beta}{\partial\bar{s}} + H\tan\varphi_*\frac{\partial\alpha}{\partial\bar{s}} + H\frac{\partial\gamma}{\partial\bar{s}} + \frac{R}{V_*}\gamma = 0, \quad \frac{\partial\xi}{\partial\bar{s}} = \gamma\cos\varphi_*. \tag{3.3}$$

The boundary conditions for the deviations ($\tau > 0$) are

$$\bar{s} = 0: \quad \alpha = \beta = \xi = 0, \quad \gamma = \gamma_0, \quad \partial\beta/\partial\bar{s} = \beta_0', \quad \bar{s} = \bar{s}_+: \quad \beta = \xi = 0. \tag{3.4}$$

The perturbations are small ($|\xi| \ll 1$ as $\bar{s} \to \bar{s}_+$). Therefore, we assume that the location of the point of contact of the jet with the solid surface does not change: $X(\tau, \bar{s}_+) = L = \text{const}$, where $\bar{s}_+ = \text{const}$. Equations (1.1) are constructed on the basis of the momentless theory, and, hence, the conjugation conditions for the axes at the jet end points, $\gamma(\bar{s} = 0) = \gamma(\bar{s} = \bar{s}_+) = 0$, are invalid here.

Let us write the perturbations as $\{\alpha, \beta, \gamma, \xi\} = \{A, B, C, E\}\exp(\lambda\tau)$, where $A(\bar{s})$, $B(\bar{s})$, $C(\bar{s})$, and $E(\bar{s})$ are the eigenfunctions of the problem and λ is the eigenvalue.

From simultaneous consideration of Eqs. (3.2)–(3.4), we obtain the following problem for the eigenfunctions:

$$A' = -B' - \lambda A/V_*, \quad C' = -\frac{R\cos\varphi_*}{HV_*}\left(B\cos\varphi_* + \frac{\cos^2\varphi_*}{H}B' + C\sin\varphi_*\right),$$
$$B'' = \frac{\lambda H}{V_*\cos\varphi_*}A + \frac{R}{V_*}\left(C\cos\varphi_* - B\sin\varphi_*\right), \quad E' = C\cos\varphi_*, \tag{3.5}$$
$$\bar{s} = 0: \quad A = B = E = 0, \quad C = C_0, \quad B' = B_0', \qquad \bar{s} = \bar{s}_+: \quad B = E = 0.$$

Here the prime denotes derivative with respect to $\bar{s}$.

Since the eigenfunctions are determined with accuracy up to an arbitrary cofactor, without loss of generality we set $B_0' = 1$.

Problem (3.5) was analyzed numerically. The values of the functions $V_*(\bar{s})$ and $\varphi_*(\bar{s})$ were found on the discrete set of points by solving problem (3.2) (by the Runge–Kutta method). The parameters H, $\bar{s}_+$, and R for the specified K and φ_{*0} values were obtained from Eqs. (2.4) (by the Simpson method).

Specifying arbitrarily λ and C_0, we solve the Cauchy problem (3.5) and determine the functions $B(\bar{s}_+)$ and $E(\bar{s}_+)$. When the specified value λ coincides with the eigenvalue of the problem, the solution of the Cauchy problem satisfies the conditions $B(\bar{s}_+) = E(\bar{s}_+) = 0$. The problem was solved by the Runge–Kutta method of the fourth order. The eigenvalue λ that ensures satisfaction of the conditions at the suction point was determined in the complex plane ($\lambda = \lambda_r + i\lambda_i$) by iteration using the parabola method.

From the eigenspectrum, we chose the least-by-modulus root that corresponded to one wavelength of the Re(B) and Re(E) disturbances for the entire jet. As a test, the small gravity deflection close to the flow of a rectilinear jet with an exponential distribution of the axial velocity was used. Thus, for $\varphi_{*0} = -\pi/48$, $R = 2.1 \cdot 10^{-4}$, and $\bar{s}_+ = 54.4$, the loss of stability occurs for $K = K^0 = 20.27$ as K increases; the frequency of neutral oscillations was $\lambda = \pm i\lambda_i = \pm i \cdot 0.2578$, where $\lambda_i = \omega^0 h/v_0$ (ω^0 is the frequency). The values obtained agree well with the results of [4] for a rectilinear jet: $K^0 = 20.22$ and $\lambda_i = \pm 0.693$ (in [4] the frequency scale v_1/l was used).

As the gravitational parameter R increases, the critical extension ratio and eigenfrequency increase. In the region studied, the dependences $K^0(R)$ and $\lambda_i(R)$ increase monotonically. With an increase in R, the designed scheme losses stability. The parameters at the boundary of the region studied are as follows: $\varphi_{*0} = -1.208$, $K^0 = 79.65$, $R = 17.22$, $\bar{s}_+ = 1.83$, and $\lambda_i = \pm 18.9$.

Figure 2 shows the calculated dependence of the critical extension ratio on the gravitational parameter (curve 6), taking into account that the parameters R and K unambiguously characterize the flow. The bifurcation (neutral) curve 6 separates the steady-flow zone with $\mathrm{Re}(\lambda) < 0$ from the unsteady-flow zone with $\mathrm{Re}(\lambda) > 0$, in which self-excited oscillations of increasing amplitude arise. The steady-flow region lies to the left of and below the bifurcation curve 6.

When in the technological process of applying a plane high-viscosity jet $K < K^0 = 20.22$, the flow is steady irrespective of the height h (the parameter R). In the forming of plane polymer films, the above parameters can vary as follows [10]: $0.1 \lesssim R \lesssim 2$ and $10 \lesssim K \lesssim 50$. Since K determines the film thickness and it is fixed in the technological process, the flow stability can be ensured by varying R. For example, let $K = 32$. According to Fig. 2, the curve 5 ($K = 32$) intersects the bifurcation curve 6 at the point $R = 1.6$. Consequently, under the condition $R < 1.6$ [relatively small distance between probe and base (h)], the flow is unsteady. An increase in h (so that $R > 1.6$) eliminates self-excited oscillations.

Thus, the gravity bending of the jet increases its stability against the occurrence of self-excited oscillations. The growth in stability with increase in R (the distance between the probe and the base) is caused by the decrease in the stretching stresses at the outlet point due to the more intense flow in the initial section under the weight of the jet. The result obtained agrees with the data on the stabilizing effect of the weight of a vertical rectilinear jet flowing downward [14].

REFERENCES

1. N. E. Kochin, *Collected Works* [in Russian], Vol. 2, Izd. Akad. Nauk SSSR, Moscow (1949), pp. 536–548.
2. A. N. Krylov, "Balance of spherical mine on a flow," in: *Izv. Min. Delu*, No. 44, 14–108 (1909).
3. V. M. Entov and A. L. Yarin, "Dynamics of free jets and films of viscous and rheologically complex liquids," *Itogi Nauki Tekh., Ser. Mekh. Zhidk. Gaza*, **18** (1984), pp. 112–197.
4. A. L. Yarin, "Occurrence of self-excited oscillations on formation of fibers," *Prikl. Mat. Mekh.*, **47**, No. 1, 82–88 (1983).
5. V. M. Entov, S. M. Mahkamov, and K. V. Mukuk, "The effect of normal stresses," *Inzh.-Fiz. Zh.*, **34**, No. 3, 514–518 (1978).
6. V. M. Shapovalov, "Bifurcation of stresses in the elongation flow of a free jet of a viscoelastic liquid," *Inzh.-Fiz. Zh.*, **60**, No. 2, 341–342 (1991).
7. V. M. Shapovalov, "Effect of various factors on the elongation flow of a free jet," Moscow (1994). Deposited at VINITI 04.13.94, No. 885-B95.
8. V. M. Shapovalov, "Unsteady flow regimes of a stretched bent polymer jet," *Izv. Ross. Akad. Nauk. Mekh. Zhidk. Gaza*, No. 3, 47–54 (1995).
9. V. E. Gul' and V. P. Dyakonova, *Physicochemical Principles of Polymer-Film Production*: Textbook for Colleges [in Russian], Vysshaya Shkola, Moscow (1978).
10. M. L. Fridman, *Processing Technology of Crystalline Polyolefins* [in Russian], Khimiya, Moscow (1977).
11. B. V. Deryagin and S. M. Levi, *Physical Chemistry of Application of Thin Layers on a Moving Base* [in Russian], Izd. Akad. Nauk SSSR, Moscow (1959).
12. A. I. Mzhel'skii, "Analysis of uniaxial elongation on rolls," in: *Rheology, Processes, and Apparatuses of Chemical Technology* [in Russian], Volgograd (1987), pp. 81–86.
13. V. M. Shapovalov and N. V. Tyabin, "Rheodynamics of elongation flow of a plane polymer jet in film stretching," *Inzh.-Fiz. Zh.*, **41**, No. 6, 1027–1031 (1981).
14. A. Zyabitskii and Kh. Kavai (ed.), *High-Speed Formation of Fibers* [in Russian] Khimiya, Moscow (1988).